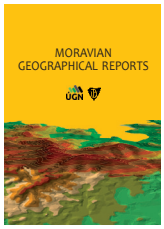

MORAVIAN GEOGRAPHICAL REPORTS

Czech Academy of Sciences, Institute of Geonics
Palacký University Olomouc, Faculty of Science

journal homepage: www.geonika.cz/mgr.html

doi: https://doi.org/10.2478/mgr-2026-0004

Analysis of triggering factors of debris flows and conditions for possible reactivation: Case study of the Lemešná Mountain in the Javorníky Range, Czech Republic

Jana Smolíková [a *], Jan Blahůt [b], Petr Tábořík [b,c], Jan Klimeš [b], Daniel Žížala [d], Vít Vilímek [a], Jan Balek [b], Filip Hartvich [b]

Abstract

On 2nd June 2010, heavy rainfall triggered a significant debris flow on the southern slope of Lemešná Mountain in the Javorníky Range (Outer Western Carpathians), Czech Republic. Multidisciplinary research was carried out there, including geomorphological survey, electrical resistivity tomography, laser scanning, soil and rainfall analysis. The debris flow occurred after the prolonged convective and intense rainfall. The antecedent precipitation index calculated for the previous 30 days reached 134.1 mm and the daily rainfall 37.4 mm, 13 times higher than the long-term average daily rainfall. The debris flow occurred in unconsolidated flysch sediments and caused minor damages. The locality was affected by slope movements in the past, as evidenced by two debris flow deposit cones in the valley. Electrical resistivity tomography revealed a sliding surface at a depth of 5 m and another at 15–20 m. However, according to local residents and the forest manager, no mass movement has been recorded in there in the last 40 years. Human intervention, particularly artificial drainage and deforestation, could also have contributed to the debris-flow triggering. The aim of this work was a complex analysis of the triggering conditions of the debris flow and a risk assessment of new events in this area.

Keywords: Debris flow, triggering rainfall, ERT, monitoring, Czech Republic

Article history: Received 10 March 2025, Accepted 6 February 2026, Published 31 March 2026

1. Introduction

Debris flows are among the most hazardous types of landslides due to their rapid movement, long runout, and destructive impact on infrastructure and ecosystems (Varnes, 1996; Jakob & Hungr, 2010). These processes are typically triggered by intense or prolonged rainfall, particularly in mountainous regions with steep slopes and susceptible geological conditions. Globally, rainfall-induced debris flows have been documented as recurrent phenomena with severe consequences for both natural environments and human settlements (Iverson, 1997; Klimeš & Vilímek, 2011; Hungr et al., 2014).

In the Czech Republic, rainfall-triggered slope deformations are a recurring hazard, especially within the flysch belt of the Outer Western Carpathians. This geologically complex region is highly prone to landslides due to its alternating layers of sandstone, shale, and claystone, which are easily weakened under saturated conditions. Flood events in 1997, 2006 and 2010 activated hundreds slope failures, including debris flows by extreme precipitation within this area (Krejčí et al., 2002; Bíl & Müller, 2008; Klimeš et al., 2009; Pánek et al., 2011a, b). The last significant debris flows in this area were recorded in September 2024 following the heavy rainfall caused by Storm Boris (September 13–16, 2024). Almost half of these debris flows were recurrent events that reactivated the same events as in 1997 (Pánek at el., 2025).

A significant case was the debris flow that occurred on 2nd June 2010 on the southern slope of Lemešná Mountain (950 m a.s.l.) in the Javorníky Range, triggered by convective rainfall. Its significance lies in its size and knowledge of the exact date and even time of its origin, which is crucial for the study of triggering factors. The failure began as a debris slide, transformed into a debris flow, and extended 340 m downslope with a source volume of 180 m^3. Although damage was relatively minor – affecting forest stands, a culvert, a forest road, and a residential building – it demonstrated the destructive potential of such processes given their velocity and sudden onset (Smolíková et al., 2021). Compared to typical shallow slope deformations in the Czech flysch belt, which measure 35–100 m in length and 20–70 m in width (Bíl & Müller, 2008), the Lemešná debris flow reached significant dimensions within the regional context, though it remains small relative to international examples.

[a] Department of Physical Geography and Geoecology, Faculty of Science, Charles University in Prague, Prague, Czech Republic (*corresponding author: J. Smolíková, e-mail: *janca.smolikova@gmail.com*)

[b] Department of Engineering Geology, Institute of Rock Structure and Mechanics, Czech Academy of Sciences, Prague, Czech Republic

[c] Department of Neotectonics and Thermochronology, Institute of rock Structure and Mechanics, Czech Academy of Sciences, Prague, Czech Republic

[d] Research Institute for Soil and Water Conservation, Soil Conservation Service – Laboratory SOWAC-GIS, Prague, Czech Republic

To date, only one study has examined the Lemešná debris flow, focusing on rainfall thresholds (Smolíková et al., 2021). Other factors – geological structure, soil properties, vegetation changes, and past slope movements – remain insufficiently explored. Moreover, the installation of a new automatic rain gauge near the site in 2012 offers an opportunity to refine rainfall analyses and improve predictive capacity for future events.

The present study therefore seeks to reconstruct the conditions that led to the 2010 Lemešná debris flow and to assess the potential for its reactivation or the occurrence of new events in the future. By integrating geomorphological field survey and mapping, orthophoto analyses, geophysical survey, soil analyses, activity monitoring, and updated rainfall data, this research aims to provide a multidisciplinary perspective on slope instability in the study area.

The main research question is whether rainfall (and what rainfall pattern) was the primary trigger of the Lemešná event, or whether other predispositions (geology, soil, mass movement history, human activity) played a significant role. Addressing this question not only enhances understanding of debris flow dynamics in the study area but also contributes to broader efforts to predict and mitigate rainfall-induced debris flows in similar geological settings.

2. Theoretical background

The origin of a debris flow depends on geological and geomorphological setting, soil conditions, vegetation cover, presence of water and human activity. It can be triggered by seismic activity, snowmelt or heavy rainfall, which is the most common cause (Sidle & Ochiai, 2006). The increasing intensity of human activities (tillage, deforestation, accelerated soil erosion, urban sprawl, improper landscape management and drainage) also contributes to the debris flow origin (Sidle, 1992; Pánek & Lenart, 2016; Muñoz-Torrero Manchado et al., 2022). Debris flow is predisposed by steep slope, unconsolidated debris material of different shapes and sizes in the source area and/or along the channel and water from some source (rainfall, lake, snow etc.) (Sidle & Ochiai, 2006).

Flysch bedrock provides particularly favourable conditions for the origin of slope deformation including debris flows (e.g. Christoulas et al., 1990; Del Prete & Guadagno, 1990; Kirchner et al., 2000; Kováčik, 1991; Pánek et al., 2009; Rączkowski, 2007). The Cretaceous–Paleogene flysch sequences consist of alternating permeable sandstones and conglomerates with impermeable shales and claystones (Bíl et al., 2014; Földvary, 1988; Pánek & Lenart, 2016). This lithological alternation, combined with rapid weathering, promotes groundwater accumulation, elevated pore-water pressures and the development of both shallow and deep-seated slope failures (Janoška, 2013; Kirchner et al., 2000; Krejčí et al., 2002; Pánek et al., 2009; Špůrek, 1972). Elements of the geological structure, such as bedding, faults and joint systems in flysch, are mainly responsible for deep-seated slope deformations, while shallow mass movements are mostly associated with heavy rainfall (e.g. Gil, 1997; Krejčí et al., 2002).

For better risk mitigation, the understanding the spatio-temporal behaviour and recurrence of slope deformations is crucial, which requires the use of different analyses. The application of geomorphological and geophysical approaches helps to study the history of slope deformations in the area, which is very important for predicting future activity (Corominas & Moya, 2008). Soil analysis shows the predisposition of the area to slope deformations and rainfall analysis helps to determine the amount of rainfall that can trigger failures (Sidle & Ochiai, 2006). Geomorphological conditions can be studied by orthophoto analyses, field survey, mapping and monitoring. Among geophysical methods, 2D electrical resistivity tomography (ERT) is a key technique because of its highest potential to reveal subsurface structures within claystone-dominated bedrock in the depths of several tens of metres (Pánek et al., 2011b). Most authors consider this geophysical technique as the most suitable for the study of the internal structure of active slope deformations (Schrott & Sass, 2008). It is used in order to show internal structure of the slope, especially structural and lithological discontinuities, identify the occurrence of the failure, its proportions, thickness and volume (Pánek et al., 2011a).

Rainfall thresholds represent a commonly used approach for identifying rainfall conditions that may trigger slope deformations. These thresholds are typically derived from individual rainfall parameters or statistical relationships between two or more parameters (Guzzetti et al., 2008; Segoni et al., 2018). A detailed analysis of the Lemešná debris flow by Smolíková et al. (2021) demonstrated that no single rainfall parameter was sufficient to explain the event. Instead, the debris flow was triggered by an exceptional combination of several short-term and long-term rainfall parameters simultaneously. Although many of the rainfall parameters that caused the Lemešná debris flow were exceeded multiple times during the 42-years of measurements, none of these exceedances occurred simultaneously across all relevant metrics. This highlights the complexity of rainfall-induced debris-flow initiation and the limitations of defining local rainfall thresholds based on a single event.

That study also provides the first rainfall values that triggered the debris flow in this locality, however, they cannot be considered as a local rainfall threshold based on a single event. No new slope deformation was recorded there between 2010–2025, but if one occurs in the future (at the same location or nearby), these values should be refined. Ultimately, the integration of geomorphological, geophysical, hydrological and rainfall analyses provide a robust framework for understanding the conditions under which debris flow originates and for improving the prediction of future hazardous events.

3. Data and methods

3.1 Study area and Lemešná debris flow

The flysch belt of the Outer Western Carpathian system has the highest density of the slope deformations in the Czech Republic. The majority of them are landslides (Krejčí et al., 2002), many of them deep-seated and reshaped by debris slides or debris flows (Pánek & Lenart, 2016). Most of the slope deformations are ancient, even numerous of them from the Pleistocene, and they are stabilised (Šilhán & Pánek, 2010). Recent events are the reactivation of old slope deformations or new landslides caused by extreme hydrometeorological situations (Krejčí et al., 2002; Pánek & Lenart, 2016; Šunka et al., 2011; Pánek et al., 2025). The main trigger in this area is long-lasting heavy rainfall (Krejčí et al., 2002; Pánek et al., 2011a). They caused floods and hundreds of landslides in the eastern part of the Czech Republic in 1997, 2006, 2010 and 2024 (e.g. Krejčí et al., 2002; Bíl & Müller, 2008; Klimeš et al., 2009; Pánek et al., 2011a, b; Pánek et al., 2025).

The area of interest of this study is located in the Javorníky Range, which belongs to the flysch belt of the Outer Western Carpathian system that was folded and thrust during the Alpine orogeny. It belongs to the Magura nappe group (Chlupáč, 2002), which is characterised by a dense trellis pattern of ridges and valleys (Pánek & Lenart, 2016). The Javorníky Range is composed of flysch bedrock. These alternating permeable and impermeable rock layers, together with deep weathering up to tens of metres, forming thick colluvium (Pavelka & Trezner et al., 2001), make the locality very susceptible mainly to shallow slope deformations in particular (Pánek et al., 2011b). The peaks of the Javorníky Range reach an altitude of about 1,000 m a.s.l. with differences

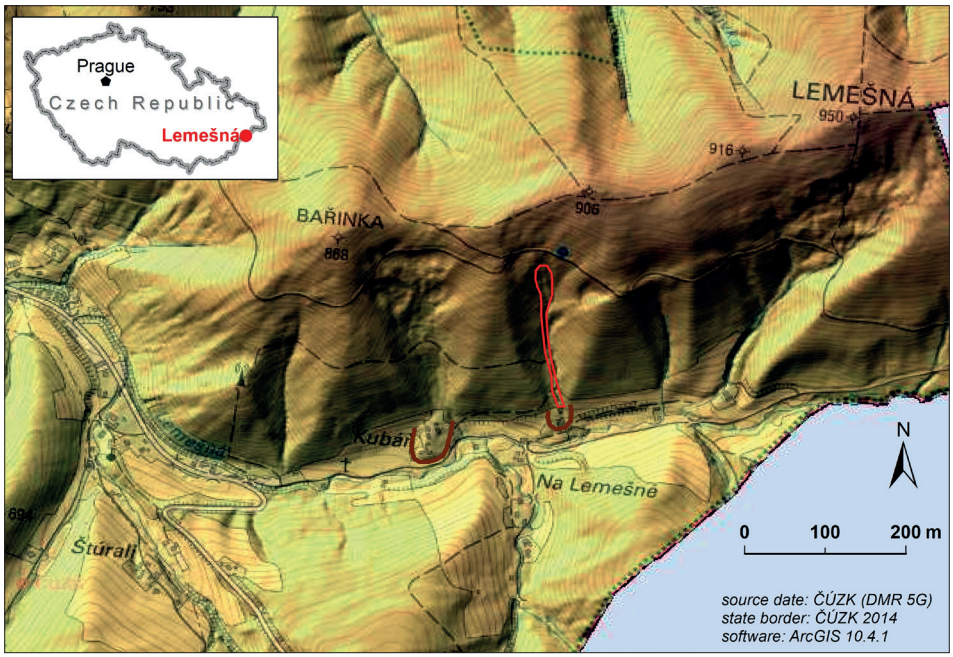

Fig. 1: The area of interest in Lemešná site with studied debris flow (red line) and deposit cones (brown lines)
Source: Authors' elaboration based on map data from the Czech Land Surveying and Cadastral Office (DMR 5G, state border)

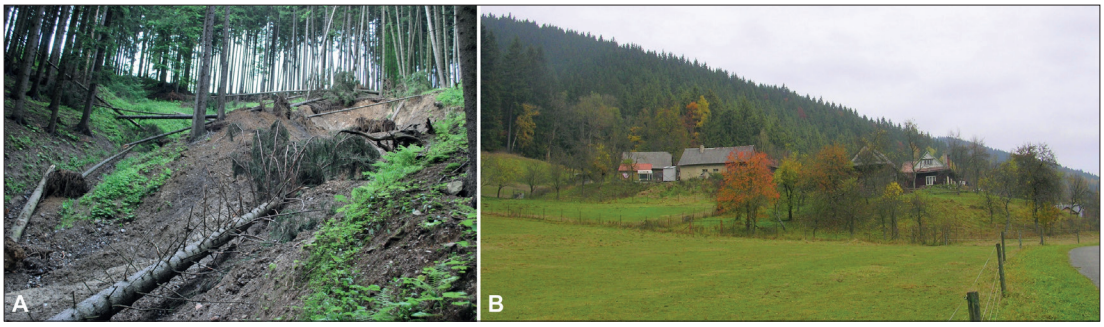

Fig. 2: (A) Source area of the investigated debris flow on the Lemešná Mt. and (B) old western deposit cone with a settlement
Photos: (A) J. Matyščák, (B) J. Smolíková

in the local relief of about 200 m. The average air temperature is about 6 °C, and the locality belongs to a slightly warm climatic region. Precipitation is heavy, the average rainfall varies between 800 and 1,000 mm per year and 300 cm of new snow (Czech Hydrometeorological Institute – CHMI).

The studied debris flow (Fig 1, Fig. 2A) is located on the southern slope of Lemešná Mt. (49.3516358N, 18.3839194E, 950 m a.s.l.), which ridge is oriented to the WSW–ENE and is bordered by the narrow Lemešná stream valley. The slopes of the ridge were affected by slope deformations in the past, which is evidenced by two distinct deposit cones (Fig. 1, Fig. 2B) that accumulated at the mouths of shallow tributary valleys with small permanent streams. The age of the deposit cones is unknown, but houses older than 100 years have been built on the western deposit cone (Fig. 2B) and houses older than 50 years on the eastern deposit cone. The slopes of the study area are covered by spruce forest, which occupied the area east of the debris flow only during in the first half of the 19th century (2nd Military Survey, Austrian State Archive, www.mapy.cz). Nevertheless, the area of forestation in the vicinity of the debris flow changed over time based on forest management needs (www.mapy.cz).

Two significant rainfall episodes were recorded in 2010 there, the first from 15th to 18th May and the second from 31st May to 2nd June (Šunka et al., 2011). These episodes caused more than 150 slope deformations of various types, including debris flows, in the flysch of the Outer Western Carpathians (Pánek et al., 2011b; Bíl et al., 2014). One of the most significant cases was debris flow (*sensu* Nemčok et al., 1972) that occurred on 2nd June 2010. It was triggered between 9:30 and 10:00 a.m. (Matyščák, commander of the fire brigade, oral communication) by intense and long-lasting convective rainfall. The slope deformation started as a debris slide with a crown width of 14 m and a scarp height of 0.8 m. After 100 m, it channelised into a stream and continued as a debris flow to a culvert and a forest road downhill, which caught most of the transported material. Only highly saturated mud reached a house on the debris flow deposit cone at the foothill. The total length of the debris flow was 340 m and the estimated volume of the source area was 180 m^3.

As we mentioned in the Introduction, the Lemešná debris flow reached significant dimensions within the regional context and showed its destructive potential. Fortunately, thanks to the remote and sparsely populated location, only relative minor damage occurred (Smolíková et al., 2021).

3.2 Orthophoto analyses, geomorphological survey and debris flow activity monitoring

An orthophoto from an aerial photography presented on the Mapy.cz website was used for remote analyses of the study area during the period 2001–2025. Attention was mainly focused on changes in the forest cover.

Field survey and mapping of the debris flow and its surroundings was carried out in 2011 and 2012, one and two years after the debris flow occurrence. A descriptive sketch was created based on it in the ArcGIS environment – ArcGIS Pro. The debris flow activity was monitored precisely between 2011 and 2014 using geodetic and laser scanning methods. An initial geodetic survey was done using a total station Leica TPS1200 in October 2011, when fixed geodetic points were installed within and around the debris flow (Fig. 3) to monitor its movement. A Terrestrial Laser Scanner (TLS) ILRIS 3D had been applied annually since 2012, once a year in the autumn, when the vegetation coverage was sparse. It allowed capturing terrain characteristics with denser data however several post-processing steps were needed to prepare the data for inter-annual comparison. In this study, the area was scanned from several sites to cover the entire area and avoid shaded zones (Abellán et al., 2014). The acquired point clouds were jointed in PolyWorks software.

In order to compare the measured data, the pointclouds were cleaned from vegetation. For this purpose, a combination of automatic and manual cleaning was performed. At first, an automatic pointcloud classification was made using Global Mapper with Lidar extension. The results were subsequently checked manually and remaining vegetation was deleted from the pointclouds using CloudCompare software. Finally, the pointcloud's distance was compared using Geomagic Studio. Subsequent ongoing monitoring was carried out by visiting the locality between 2015 and 2025.

3.3 Electrical resistivity tomography

The subsurface structure of the area of interest was investigated by electrical resistivity tomography (ERT). The measurement was carried out by means of the multi-electrode ARES system (GF Instruments, Czech Republic), the Wenner-Schlumberger electrode array. Obtained ERT data were processed in Res2Dinv software (Geotomo Software) using inverse modelling (least square inversion) with finite-element optimisation and default dumping factor. Final inverted resistivity models were calculated from apparent resistivity values and displayed in form of pseudosections (tomographic sections) in Res2D/3Dinv software (Loke, 1997). The most erroneous data were adjusted by means of root-mean-square (RMS) error statistic (RMS error cut-off). Maximum RMS error of the inverse model was 19.8% in the profile LEM3 (Fig. 3) which can be still considered as a reliable result in conditions of the anisotropic flysch bedrock. Topography was introduced directly into the inversion process.

Geophysical survey on the Lemešná site included longitudinal profile LEM1 (Fig. 3) across the 2010 debris flow. Profile LEM3 was conducted in prolongation of the original profile LEM1 to the NNW direction (reaching the mountain ridge). LEM1 and LEM3 were jointed into the profile LEM1-3 with 151 m overlap. Transverse profile LEM2 intersected perpendicularly the LEM1-3 at 270 m. Profile LEM4 was situated parallelly to the joint-profile LEM1-3 to depict subsurface situation outside (but close enough to) the active slope deformation. Profile LEM5 was carried out across the old deposit cone in distance of approximately 180 m downslope from the 2010 debris flow accumulation. Selected parameters of the ERT survey are summarised in Table 1 and situation of the individual profiles is marked in Figure 3.

Profile	Length [m]	Electrode spacing [m]	Approximate max. depth [m]	Profile orientation
LEM1*	285	3	ca. 60	longitudinal
LEM2	206	2	ca. 40	transverse
LEM3*	285	3	ca. 60	longitudinal
LEM4	309	2	ca. 65	longitudinal
LEM5	142	2	ca. 30	transverse

*Tab. 1: Selected parameters of the 2-D ERT survey at the Lemešná site (Note: *Profiles LEM1 and LEM3 were interpreted together as the integrated profile LEM1-3 with total length of 419 m (and with 151 m overlapping)*
Source: Authors' survey and elaboration

3.4 Soil samples analysis

Soil samples were taken above the debris flow head scarp due to the distinct soil layers in depths of 7, 15, 28 and 40 cm. Additional one sample was taken 5 m higher from the depth of 10 cm. Physical and index soil properties were determined from these samples to describe soil predisposition to slope deformation (Myslivec et al., 1970; Atkinson, 2007). Soil moisture conditions, liquid limit, plasticity limit and grain size distribution were measured in certified laboratory GEMATEST Ltd. Geomechanics Laboratory in Prague due to standard procedure of Czech State Standards and methodology of laboratory tests (Zavoral et al., 1987).

Soil moisture was determined due to the Czech State Standard CEN ISO/TS 17892-1 (2015) by soil sample drying in an oven at 105 ± 5 °C for 24 hours. Afterwards the sample was placed in a desiccator to getting cool. The soil sample was weighed before and after the oven-drying and finally, the moisture content was calculated and expressed as a percentage. Uncertainty of measurement was 0.2% (GEMATEST Ltd.). Atterberg's limits were determined due to the Czech State Standard CEN ISO/TS 17892-12 (2005). Liquid limit was tested mechanically by Casagrande cup's test at which two sides of a groove came close together for a distance of 12.7 mm under the impact of 25 number of blows and plasticity limit was determined by rolling out a thread of soil of 3 mm in diameter on a flat surface. Grain size distribution was set due to Czech State Standard CEN ISO/TS 17892-4 (2005) by the combination of sedimentation test in hydrometer and sieve analysis with 8% of the uncertainty of measurement (GEMATEST Ltd.).

Consequently, plasticity index, consistency index, angle of internal friction, cohesion and cohesion at higher saturation were derived from Czech State Standards 731001 (1988).

3.5 Rainfall data and analyses

The nearest rain gauge in the vicinity of the study area is Velké Karlovice – Pluskovec (VKP). It is situated 7 km west from the debris flow at an altitude of 561 m a.s.l. The rain gauge is located in different orographic conditions than the debris flow, thus the exact amount of rainfall, which precipitated during the event, is not exactly known. The VKP, managed by CHMI, has measured daily cumulated rainfall amounts every day at 7:00 a.m. since 1983. A new automatic rain gauge Lemešná (LEM) with detailed data recording (10-minute interval) was installed close to the foot of the debris flow slope at 678 m a.s.l. in 2012.

Detailed analysis of triggering rainfall was carried out by Smolíková et al. (2021). The rainfall data from the VKP was analysed in the period from 1st January 1983 to 31st December 2018 (with data outage between 1st December 1986 and 31st March 1987) and from LEM in the period from 29th June 2012 to 16th July 2016. In this study, this series of rainfall data was updated and extended to cover the period from 1st January 1983 to 19th October 2025 in the VKP (with the same outage) and 29th June 2012 to 16th August 2024 in LEM (with data outage between 17th July 2016 and 2nd December 2018).

Antecedent Precipitation Index (API), cumulative sum of the rainfall totals (CUM) and daily rainfall totals were analysed for the VKP measurements for the period 1/1983–10/2025. The API shows the precipitation situation retrospectively and it is used to define the antecedent moisture conditions (Mishra & Singh, 2003). The CUM sums the rainfall for the previous days regardless of

evapotranspiration or runoff. For the purposes of this study the API and CUM were calculated for a floating number of 5, 10, 15, 20, 30, 60 and 90 days (n = 5, 10, 15, 20, 30, 60 and 90). The applied equation of API (Kohler & Linsley, 1951) is:

$$API_n = \sum_{i=1}^{n} c^i \times P_i \quad [\text{mm}]$$

where n = the total number of days prior to the causal rainfall, i = the number of days counting backwards from the date on which the API is determined, c = an evapotranspiration constant (c = 0.93 is used for the Czech Republic – Steinhart, 2010), and P_i = the amount of precipitation i days prior to the causal rainfall [mm].

Also, available rainfall data from LEM was compared with data from the VKP during the period 2012–2024.

4. Results

4.1 Geomorphological and forest conditions and recent activity of the debris flow

The debris flow originated on the Lemešná Mt. at an altitude of 820 m a.s.l. on a slope with average inclination of 35°. The debris flow's length reached 340 m, width varied from 4–14 m in the source zone and 35 m in the middle part, scarp height reached 0.8 m. Estimated volume of the source area was 180 m^3. The first part of the transport zone passed on the hillside surface while the second run in the stream bed where the transported material left two minor accumulations on locally narrowed sites (Fig. 3). It stopped at culvert below the forest road in the lower part of the slope. The culvert was clogged and vast majority of the transported material was deposited there while only flood with finer particles continued further downstream reaching the buildings on the eastern deposit cone and the valley floor.

Evidence of ancient mass movement activity was identified in the whole valley of the Lemešná stream. The most noticeable marks are two old deposit cones in the valley floor. Apart from this, there are many small inconspicuous scarps and accumulations overgrown with dense forests. Old scarps were found in the close vicinity as well, next to the 2010 debris flow and in the upper slope part above the road (Fig. 3), which was cut down recently. Also, considerable 25 m long active tension crack with scarp up to 0.3 m high has developed above the source area.

In the hillside rise several springs and flow streams for the most of the year which supply the main stream in the lower part. Occurrence of the spring in the hillside above the debris flow, next to the forest road (Fig. 3), could have significantly contributed

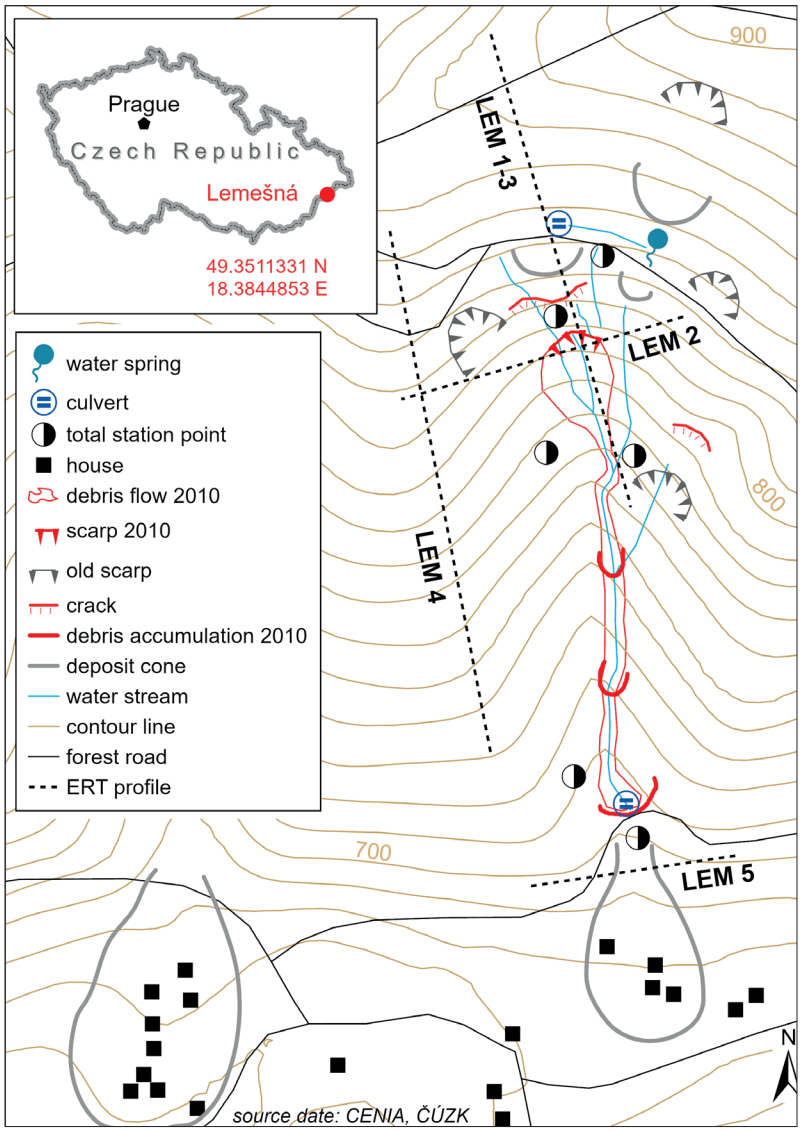

Fig. 3: Sketch of the Lemešná debris flow and its surroundings with ERT profiles
Source: Authors' elaboration based on map data from the Czech Land Surveying and Cadastral Office (contour line, state border) and Czech Environmental Information Agency (topography)

to the debris flow activation as well. Water from the spring has been drained by a road ditch and after 15 m deviated in the culvert under the road into the debris flow slope.

On the basis of orthophoto, changes in the forest cover were observed. Approximately 2.5 ha of mature forest were cut down above the road above the debris flow between 2003 and 2006 (Fig. 4A, B). Another 1.2 ha was cut down between 2006 and 2010 (Fig. 5B, C). These changes in forest cover could have caused significant changes in runoff conditions on the slope above the debris flow and contributed to its origin.

Differential terrain models derived from the laser scanning showed that larger changes in terrain shape occurred between 2012 and 2013 (Fig. 6A). After this period the surface change decreased. It is clearly visible that negative mass balance occurred mostly in ravines (blue colours), while some material gain (orange colour) was observed in the upper sector and on two ridges in the debris flow bottom. A significant crack in the central part of the surveyed area was well recognisable as well. Since 2015, there has been no significant landslide activity in this area and the debris flow site is gradually becoming overgrown with planted vegetation (Fig. 5D).

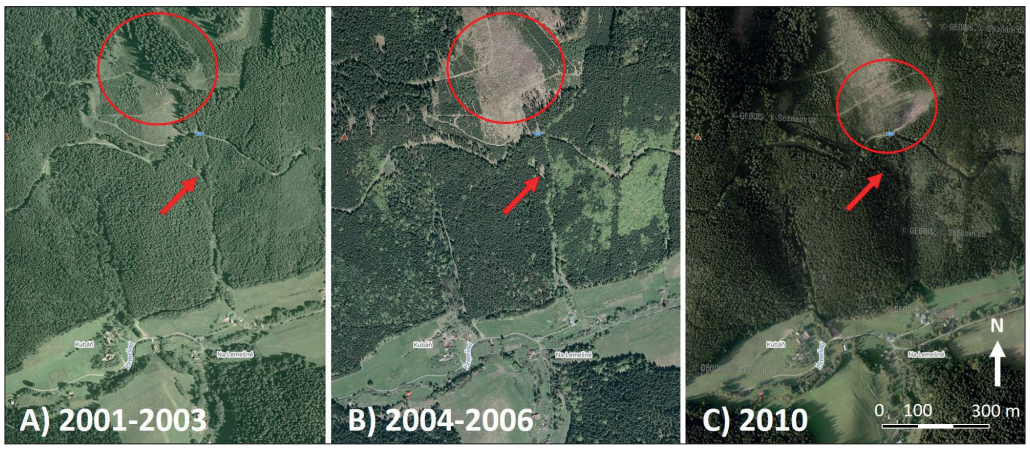

Fig. 4 Changes in the forest cover (red circle) of slope above the debris flow (red arrow) during 2001–2010
Source: Authors' elaboration based on map data from Mapy.cz

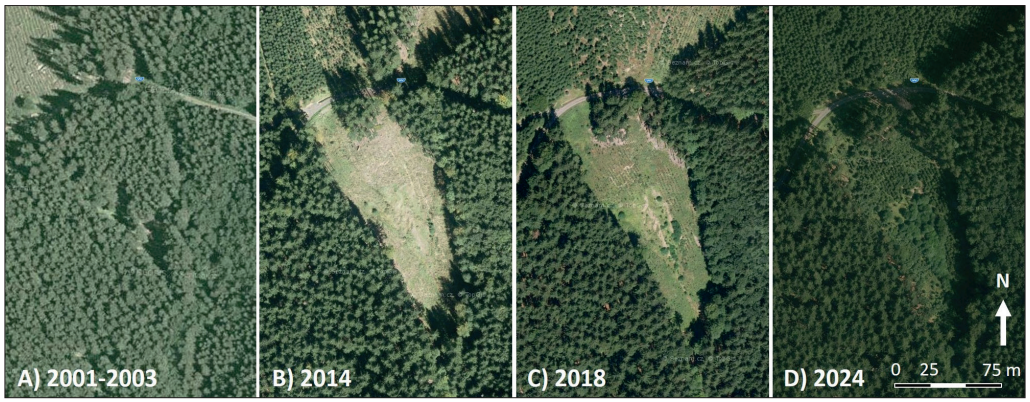

Fig. 5: Changes in the forest cover at the site of the debris flow during 2001–2024
Source: Authors' elaboration based on map data from Mapy.cz

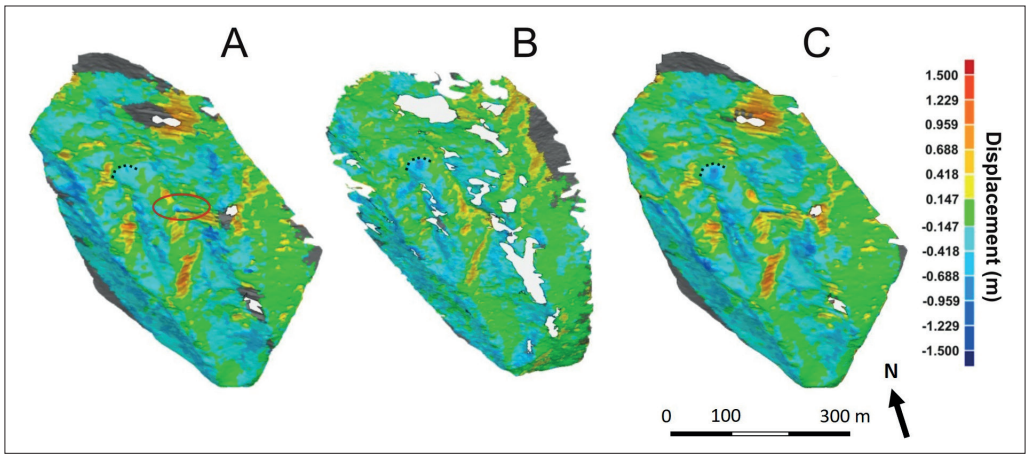

Fig. 6: Differential terrain models from TLS survey comparing area in 2012, 2013 and 2014. (A) Comparison between 2012 and 2013, (B) comparison between 2013 and 2014 (C) comparison between 2012 and 2014; (negative values indicate areas with loss of material while positive values indicate positive material balance; the black dotted line represents the debris flow's scarp; red oval marks the crack)
Source: Authors' survey and elaboration

4.2 Internal structure of the study area

The joint-profile LEM1-3 with total length of 419 m depicted subsurface situation above and across the studied debris flow (Fig. 7). It showed the alternating subvertically borderlines (dipping at ca. 40–60°) heterogeneous anisotropic flysch rock formations (the depth up to 30 m). Relatively higher values of resistivity (> 80 Ω.m) stand for sandstone-dominated flysch layers (s), while lower resistivity values (< 80 Ω.m) represent higher occurrence of the fine-grain sedimentary rocks, i.e. claystones or siltstones (marls?) (c). Profile LEM1-3 probably did not cut the layers perpendicularly, but obliquely. Therefore, the layers may appear thicker than they are. Low resistivity (< 80 Ω.m) of water saturated zone represents active shallow mass movement (2010 debris flow) with maximum depth up to 5 m; from 250 m to 365 m on the LEM1-3 profile (Fig. 7). A possible other slope deformation is indicated underneath of the current debris flow with sliding plane at depth of ca. 15–20 m. Also, is possible to distinguish a distinct horizontal resistivity gradient (vertical boundary) on ca. 270 m, likely tectonic fault.

The longitudinal profile LEM4 (Fig. 7) was carried out to reveal the subsurface situation outside the debris flow zone parallel with the profile LEM1-3. The resistivity pseudosection shows

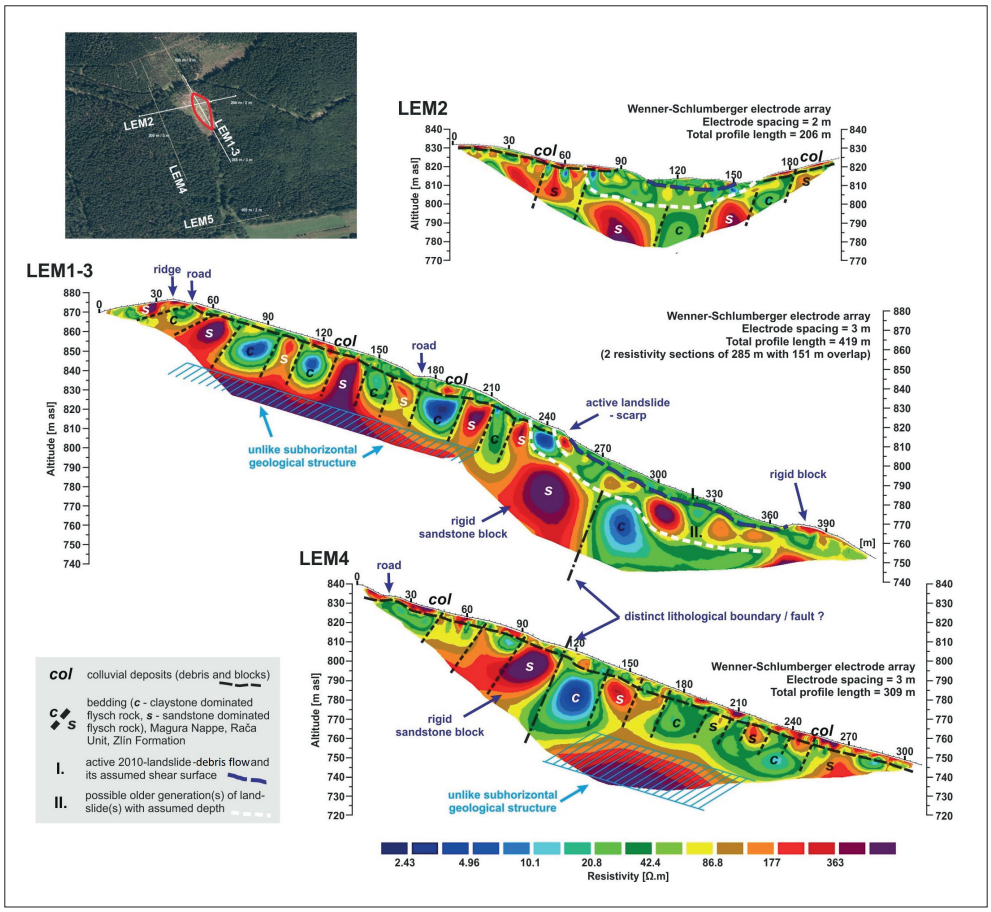

Fig. 7: Resistivity inverse models with topography – profiles LEM1-3 (joint-profile), LEM2 and LEM4 representing subsurface resistivity distribution with structure-geological and geomorphological interpretations (inserted ortophoto cut-out displays the situation of the ERT profiles; red oval represents the debris flow)
Source: Overview ortophoto map – authors' elaboration based on map data from Mapy.cz; ERT profiles – authors' survey and elaboration

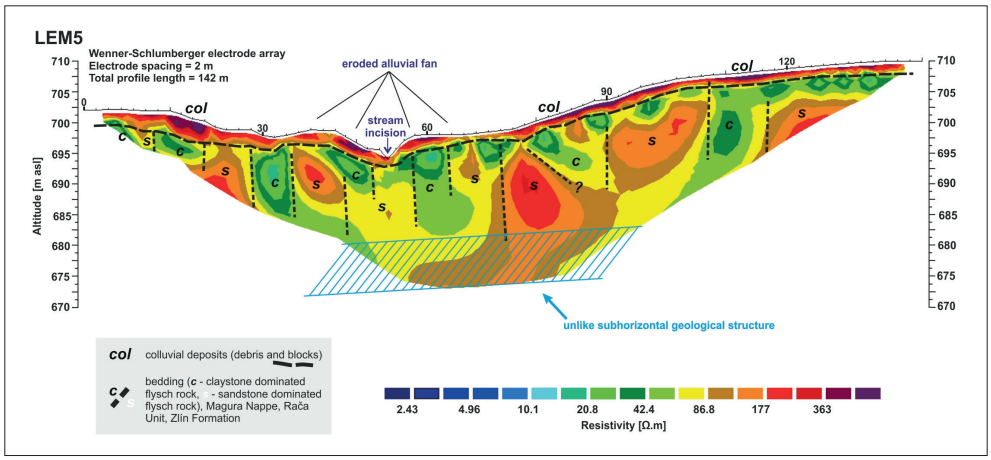

Fig. 8: Resistivity inverse model with topography – profile LEM5 displaying eroded alluvial fan and subsurface structure-geological situation of subvertically inclined alternating flysch rock formations (localisation of the profile is marked in Fig. 3)
Source: Authors' survey and elaboration

very similar characteristics as in the profile LEM1-3, comprising of alternating subvertically layered heterogeneous flysch rocks, colluvial (weathered) mantle and, also, the above-mentioned vertical resistivity boundary, likely fault, on ca. 110 m of the profile. The ERT profile LEM2 (Fig. 7) displayed the situation transverse across the investigated debris flow scarp. Both above-described sliding planes (at depth of 5 m and 15–20 m) are distinguishable too. Also, subvertical layering of the flysch formations is preserved. Based on the position of the displayed layers in longitudinal and transversal profile, it can be assumed that the layers are formed with inclination of ca. 40–50° from the longitudinal axis of the slope. LEM5 (Fig. 8) resistivity section displayed eroded alluvial fan and sediments up to 3 m thick with relatively high values of resistivity (> 100 Ω.m).

4.3 Soil properties

Soil samples analyses (Tab. 2) showed a low percentage of moisture, less than 20% in all samples, decreasing with depth. Grain size distribution showed very high content of the fine-grain material (clay and silt), that is more susceptible to debris flow type mass movement. Samples no. 2, 4 and 6 had > 70%, sample no. 3 had 52% of fines while sample no. 5 had the lowest content (27%).

The plasticity index, calculated from the liquid limit and plasticity limit, resulted as medium plasticity (< 20%) for two samples and high (> 20%) (Burmister, 1940) for three cases. Consistency index, which is influenced by current moisture, came out greater than 1 in all samples, thus the soil was rather strong (Atkinson, 2007). On the other hand, cohesion and cohesion at higher saturation was really small (Myslivec et al., 1970).

Angle of internal friction was in all cases smaller than slope dip of the sampling site pointing out the importance of cohesion and suction in the stability of the slopes.

4.4 Rainfall effect on the debris flow triggering

The rainfall data series from the VKP was updated, extended and analysed to cover the period from 1st January 1983 to 19th October 2025 (with data outage between 1st December 1986 and 31st March 1987). And the rainfall data from LEM was updated to cover the period 29th June 2012 to 16th August 2024 (with data outage between 17th July 2016 and 2nd December 2018).

Rainfall totals of 320.6 mm were recorded in the study area in May 2010, which was 3 times higher than long-term monthly average for May (93.6 mm, CHMI). Moreover, two heavy rainfall episodes occurred there. The first on 15th–17th May 2010, when one third of monthly rainfall total fell. Soil became saturated and afterwards the second rainfall wave arose on 30th May–1st June 2010.

The debris flow originated on 2nd June 2010 between 9:30 and 10:00 a.m. (Matyščák, commander of the fire brigade, oral communication) after the daily rainfall total of 37.3 mm the day before. This amount was 13 times higher than the long-term daily average amount (2.7 mm, CHMI), but not the highest for the examined period 1983–10/2025 (Fig. 9).

Analysis of the Antecedent Precipitation Index showed, that API30 reached 134.1 mm the day before the debris flow. This volume was among the 33 highest API30, occurring during only six rainfall events over the 42-year measurement period –

Analysis		Number of samples				
		2	3	4	5	6
Depth of the sample [cm]		7	15	28	40	10
Sample locality		head scarp	head scarp	head scarp	head scarp	above head scarp
Moisture [%]		19.6	18.9	13.3	10.4	18.8
Liquid limit [%]		55	48	36	49	54
Plasticity limit [%]		35	33	24	29	31
Plasticity index [%]		20	15	12	20	23
Consistency index		1.77	1.94	1.89	1.93	1.53
Granularity [%]	clay	16	21	17	13	31
	silt	57	31	54	14	46
	sand	5	32	5	19	15
	gravel	22	16	24	54	8
Angle of internal friction [°]		16	26	18	32	16
Hillslope angle [°]		42	42	42	42	36
Cohesion [kPa]		12	16	16	0–4	12
Cohesion at higher saturation [kPa]		5	10	9	–	5

Tab. 2: Results of soil sample analyses (processed in the certified laboratory GEMATEST Ltd. Geomechanics Laboratory in Prague)
Source: Authors' survey and elaboration

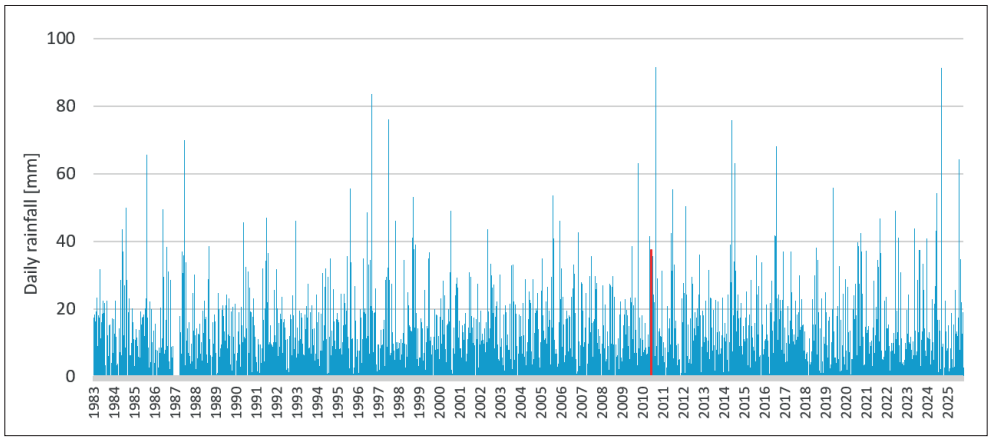

Fig. 9: Daily rainfall during 1/1983–10/2025 at VKP rainfall gauge (red line – rainfall data preceding the debris flow)
Source: Authors' elaboration based on rainfall data from the Czech Hydrometeorological Institute

in 1985, 1996, 1997, in the first part of May 2010 and 2024 (Fig. 10). The year 1997, with extreme flooding rainfalls, had the same trend as 2010, with two heavy rainfall episodes, moreover, the first episode was much heavier than in 2010. API analyses for 60 and 90 days showed the same trend (graph curve) as API30 with extreme totals on the same days, just with one more extreme day, so that the debris flow day resulted in the seventh highest volume with rainfall totals of 137.5 mm for 60 days and 137.8 mm for 90 days.

Despite these results, the 2010 debris flow was the only recorded slope deformation event within the study area and the analysed 42-year period (1983–2025). No new slope deformation has been recorded since 2010, even though the updated rainfall data from 2018–2025 showed higher values for several rainfall parameters than those recorded during the debris flow event. This may be attributed to the fact that all calculated rainfall parameters together peaked on the day preceding the debris flow. Throughout the entire 42-year measurement, these parameters never reached comparable values simultaneously on the same day (Tab. 3).

The results also confirmed significant differences in rainfall totals at the VKP and LEM rainfall gauges (Tab. 4). Although the gauges are only 7 km apart, rainfall amounts in a mountainous environment can vary significantly even over such a short distance.

5. Discussion

According to Klimeš (2007), about 70% of the new mass movements are located within 75 m from the ancient mass movements. Previous mass movement activity, such as two old deposit cones at the bottom of the valley, many recent scarps, cracks and accumulations were found in the study area. In addition, a small shallow mass movement observed in the western upper part of the study area, which flows into the debris flow, may have facilitated its formation.

Another contributing factor was a water spring that rose from the upper slope above the forest road and is located right next to the road (Fig. 3). Its water was channelled through a ditch along the road and discharged into the culvert below the road directly into the affected slope. This made the subsurface flow stronger and more concentrated (Sidle & Ochiai, 2006). The excessive volume of water from the rainfall and the spring in the slope could be strong enough to contribute to the 2010 debris flow. Also, the long-term repeated water fluctuations in the soil, which progressively reduced the soil strength, the process called hydro-mechanical fatigue (Preisig et al., 2016), could have played an important role. As a result, the debris flow could occur during rainfall that was not extreme, but heavy enough to overcome the soil strength that had been reduced by previous events.

Deforestation of the upper part of the slope, as in the case of the Lemešná slope, is a common cause of slope deformation including debris flows all over the world (Tsukamoto, 1990; Sidle, 1992; Sidle & Ochiai, 2006; Muñoz-Torrero Manchado et al., 2022). Timber harvesting reduces soil cohesion and modifies the soil moisture regime through evapotranspiration. It can also increase soil erosion rate, even two to ten times faster, especially in steep terrain with shallow and wet soils. The window of susceptibility for slope deformation occurrence after clear-felling and prior to significant regeneration ranges from about 3–15 years (Sidle, 2010). Therefore, this human intervention could also have contributed to changing the hydrological properties of the soil and contribute to the debris flow origin.

The terrestrial laser scanning monitoring has not shown any significant debris flow activity since 2012. Minor loss of material in the scarp and gullies caused by gradual rill and gully water erosion was observed between 2012 and 2013, whereas gain of material in the upper part of the slope caused by crack erosion was monitored between 2013 and 2014 (Fig. 6B). A significant crack noted in the central part of the survey area (Fig. 6A, C) and not visible in the next year's comparison (Fig. 6B) could be caused by two things: firstly, there was some unsurveyed area in the immediate vicinity of the crack; secondly, the crack opened in 2013 and remained in place until 2014, but the area under the crack did not show any

Date	VKP [mm]	LEM [mm]	Difference [mm]
24 Feb 2013	2.1	40.0	37.9
26 May 2014	75.8	4.8	71.0
31 Jul 2014	7.2	41.6	34.4
22 May 2019	55.8	0.0	55.8
3 Aug 2020	39.7	0.0	39.7
19 Aug 2020	38.6	0.0	38.6
25 Sep 2020	42.3	0.0	42.3
31 Aug 2021	46.7	0.0	46.7
9 Jul 2022	49.0	3.2	45.8
30 Nov 2022	0.0	35.0	35.0
16 May 2023	43.8	4.4	39.4
17 May 2023	2.9	41.0	38.1
12 Dec 2023	1.2	37.0	35.8
1 July 2024	54.2	0.0	54.2

Tab. 4: Maximum recorded difference in daily rainfall in the VKP and LEM rainfall gauge
Source: Authors' calculations and elaboration based on rainfall data from the Czech Hydrometeorological Institute (VKP) and from our own rainfall rain gauge (LEM)

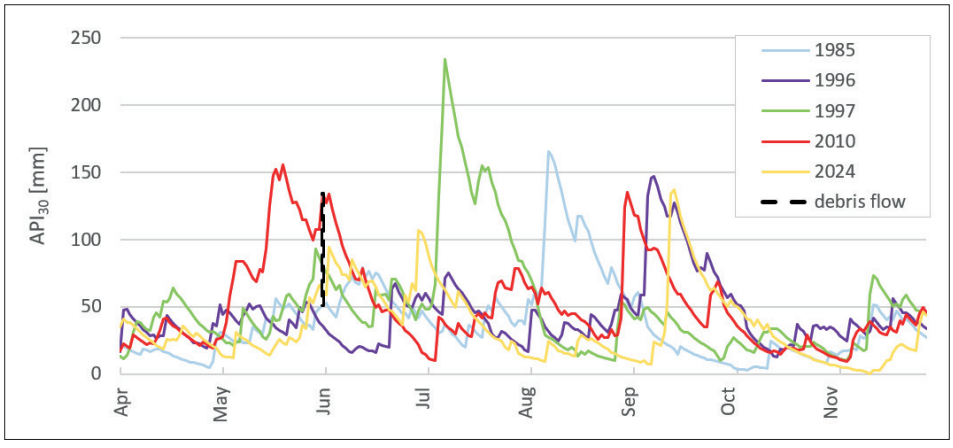

Fig. 10: API30 of rainfall data at VKP rainfall gauge higher than debris flow 2010 amounts during 1/1983–10/2025 (black dashed line – debris flow occurrence)
Source: Authors' calculations and elaboration based on rainfall data from the Czech Hydrometeorological Institute

Year	Month	Day	1 day	CUM 2	CUM 3	CUM 5	CUM 10	CUM 15	CUM 20	CUM 30	CUM 60	API 5	API 10	API 15	API 20	API 30	API 60
1985	8	7	58.0	69.1	69.1	84.6	118.5	118.5	164.4	186.1	297.2	75.1	95.9	95.9	108.5	112.4	116.5
1985	8	8	65.5	123.5	134.6	150.1	184.0	184.0	229.9	251.6	354.1	130.8	150.1	150.1	161.9	165.4	169.2
1985	8	9	9.5	75.0	133.0	144.1	186.8	193.5	219.2	261.1	352.4	120.4	145.4	148.4	155.0	162.7	166.1
1985	8	10	5.3	14.8	80.3	149.4	187.9	198.8	213.9	266.4	357.7	116.9	138.2	142.9	146.7	156.2	159.4
1985	8	11	0.0	5.3	14.8	138.3	187.9	198.8	213.9	266.4	353.5	101.6	128.6	132.9	136.5	145.3	148.2
1985	8	12	0.0	0.0	5.3	80.3	164.9	198.8	198.8	266.4	335.2	56.9	109.2	123.6	123.6	135.1	137.6
1986	6	5	49.5	55.9	55.9	78.4	113.4	137.1	150.0	168.6	206.0	67.2	86.5	95.3	99.0	102.0	103.3
1987	6	26	70.0	70.0	93.8	93.8	103.4	170.0	184.9	230.0	386.2	84.2	89.7	117.1	120.8	128.7	137.3
1996	9	7	83.5	88.5	108.3	109.3	135.1	158.7	180.6	205.4	268.6	98.7	112.4	122.7	128.6	132.5	136.1
1996	9	8	24.0	107.5	112.5	133.3	155.3	182.7	204.6	229.4	292.0	114.1	125.1	136.4	141.9	145.6	148.9
1996	9	9	12.7	36.7	120.2	145.0	151.5	194.7	217.3	242.1	303.7	117.2	120.8	138.5	143.8	147.2	150.2
1996	9	10	3.3	16.0	40.0	128.5	153.3	198.0	199.8	245.4	304.0	99.3	114.7	131.8	132.3	140.0	142.8
1997	7	6	76.0	96.5	103.5	107.5	127.8	155.2	200.1	209.6	382.7	97.0	109.5	118.9	130.0	131.9	139.4
1997	7	7	70.0	146.0	166.5	177.5	196.5	204.0	237.9	279.6	424.2	155.3	166.4	169.0	179.0	187.8	194.4
1997	7	8	63.8	133.8	209.8	237.3	260.3	262.3	301.7	342.7	488.0	201.2	214.0	214.8	225.8	233.9	240.2
1997	7	9	0.6	64.4	134.4	230.9	260.9	262.2	296.6	343.3	488.6	183.2	199.6	200.1	209.3	218.1	223.9
1997	7	10	0.0	0.6	64.4	210.4	250.9	262.2	289.6	343.3	488.6	157.1	181.1	186.1	193.1	202.8	208.2
1997	7	11	0.0	0.0	0.6	134.4	241.9	262.2	289.6	343.3	488.6	96.9	164.4	173.1	179.6	188.6	193.7
1997	7	12	1.6	1.6	1.6	66.0	243.5	262.5	270.0	344.9	490.2	46.3	154.4	162.1	163.9	176.9	181.6
1997	7	13	4.5	6.1	6.1	6.7	244.0	267.0	269.0	349.4	494.7	6.0	146.0	154.9	155.4	168.7	173.1
1997	7	14	0.0	4.5	6.1	6.1	237.0	267.0	268.3	346.3	494.7	5.2	132.6	144.0	144.4	156.6	160.9
1997	7	15	0.0	0.0	4.5	6.1	216.5	257.0	268.3	346.3	486.7	4.8	114.1	130.8	134.3	145.6	149.6
1997	7	16	0.0	0.0	0.0	6.1	140.5	248.0	268.3	340.6	469.7	4.5	71.9	118.9	124.9	134.8	138.9
1997	7	19	23.2	51.7	56.3	56.3	62.4	293.3	323.3	359.0	510.1	49.9	53.5	142.2	150.1	154.8	161.5
1997	7	20	8.3	31.5	60.0	64.6	70.7	281.1	321.6	360.3	504.4	54.1	57.5	133.5	145.2	151.0	157.7
1997	7	21	14.0	22.3	45.5	78.6	84.7	219.1	326.6	374.3	512.8	63.4	66.5	113.4	146.1	153.4	159.6
1997	7	22	1.9	15.9	24.2	75.9	85.0	151.0	328.5	355.0	514.2	57.7	62.9	85.3	137.6	142.2	150.2
1998	9	15	53.0	56.1	83.2	124.4	131.1	140.4	151.2	181.6	251.3	104.6	107.8	112.0	115.4	120.5	123.0
2005	8	24	37.8	78.5	95.6	96.2	102.0	124.5	136.3	204.5	312.2	84.5	87.4	96.0	99.4	113.3	117.5
2010	5	16	41.6	66.2	70.8	90.6	108.3	188.7	201.1	208.0	276.7	78.3	87.6	120.0	123.7	124.9	129.3
2010	5	17	33.7	75.3	99.9	120.7	135.5	218.2	234.6	241.7	310.4	101.8	109.9	141.6	146.3	147.5	151.6
2010	5	18	16.0	49.7	91.3	120.5	145.7	221.0	250.6	256.5	326.4	99.1	114.4	142.5	151.0	152.0	155.8
2010	5	19	3.2	19.2	52.9	119.1	145.9	200.0	253.8	259.7	329.6	92.2	108.1	127.9	143.4	144.3	147.9
2010	5	20	23.0	26.2	42.2	117.5	166.5	202.2	268.0	281.2	349.1	91.2	120.8	133.8	152.8	155.4	158.9
2010	5	21	0.3	23.3	26.5	76.2	166.8	184.5	264.9	281.5	349.4	58.2	112.6	119.1	141.6	144.8	148.1
2010	5	22	2.1	2.4	25.4	44.6	165.3	180.1	262.8	283.6	351.5	34.2	105.1	110.7	132.8	136.6	139.6
2010	**6**	**1**	**37.3**	**45.9**	**63.1**	**63.3**	**87.5**	**132.1**	**252.8**	**350.3**	**423.2**	**56.1**	**70.1**	**86.6**	**120.9**	**134.3**	**137.5**
2010	8	31	91.5	107.5	110.8	120.0	128.8	133.8	150.3	179.2	341.1	108.0	113.1	114.9	119.6	124.0	131.7
2010	9	1	21.0	112.5	128.5	131.8	149.8	152.9	171.3	200.2	362.1	114.0	124.7	125.8	130.8	134.8	142.0
2019	5	22	55.8	75.2	80.4	86.4	95.5	116.0	132.8	176.8	186.9	77.3	82.2	90.5	94.7	102.3	102.7
2022	6	9	49.0	68.1	86.1	86.1	101.6	105.8	112.6	138.5	188.3	76.6	85.2	87.0	89.0	93.5	96.5
2024	6	30	54.2	54.2	73.6	102.3	105.5	113.6	124.3	203.4	320.5	86.1	87.7	90.5	93.8	106.5	114.0
2024	9	14	91.2	117.7	129.3	129.8	150.7	151.3	151.4	174.9	206.5	117.4	130.6	130.9	130.9	134.0	135.6
2024	9	15	13.2	104.4	130.9	142.5	163.9	164.4	164.5	188.1	219.7	121.1	133.8	134.0	134.0	136.9	138.3
2025	7	27	64.3	71.4	72.1	80.2	98.5	133.6	176.1	193.7	246.5	72.6	83.0	97.0	107.9	111.5	113.6

Tab. 3: Selected calculated rainfall parameters (mm) of the extraordinary rainfall episodes exceeding the rainfall totals of the 2010 debris flow day
Notes: red highlighted – exceeding values; bold and blue frame – the debris flow values; Storm Boris – September 13–16, 2024
Source: Authors' calculations and elaboration based on rainfall data from the Czech Hydrometeorological Institute

significant gain material during the survey period. Many unstable landforms were left after the 2010 debris flow, so the recorded material movement within the monitored area was caused by surface erosion and gravity. Gaps in the analysed data were caused by dense vegetation that had colonised the debris flow since 2013 and had to be removed from the analysed point clouds. As the debris flow did not show any significant activity, it was decided to stop scanning and observe the site visually only.

ERT showed subsurface situation below the debris flow, where the subvertically layered heterogeneous anisotropic flysch rock formations were found, which represent a high susceptibility of the slope deformations (Lenart et al., 2014; Pánek et al., 2014; Šilhán & Pánek, 2010; Tábořík et al., 2017), were found. Furthermore, two sliding surfaces were clearly distinguished. The shallower one, the 2010 debris flow at a depth of 5 m, and the second, situated just underneath the debris flow at a depth of 15–20 m. This possible sliding plane correlates well with the tension crack formed above the debris flow detachment area and most likely indicates another slope deformation in the initial state, which is probably temporarily inactive. This is an important finding showing that more deep-seated landslide may develop in this place in the future. Regarding the knowledge about the study site and from other recent landslides (e.g. Klimeš et al., 2009; Pánek et al., 2011b) scenario of future landslide development may be formulated. In the worst case, a complex landslide would develop with sliding in its upper part which will soon transform into debris flow which may have long run-out and possibly cause damage of the houses located at the deposit cone. The 2010 debris flow with the volume of 180 m^3 caused small damages, but based on the experiences from the Czech Republic (Klimeš et al., 2017) it may have much more destructive consequences if its accumulation would not be stopped by the forest road culvert. High degree of risk imposed by this slope deformation type illustrates an event from 2013 with volume of only 90 m^3 which caused two casualties in the western part of the Czech Republic (Klimeš et al., 2017).

A distinct horizontal resistivity gradient (vertical boundary) detected by ERT could point out a lithological boundary or even tectonic rupture – possible fault. The boundary seems to be continuous and it follows on ERT profiles LEM1-3 on ca. 270 m and LEM4 on ca. 110 m, however, it has no significant morphological expression. On the other hand, clearly visible in the slope morphology is a linear feature running in NE–SW direction crossing the LEM1-3 profile in place labelled as 'rigid block'. Due to low depth reached of the ERT profiles it is not well visible on them, but it can be traced for about 750 m on the slope. It may be assumed, that both of these features represent important lithological or tectonic boundary, that may further weak the bedrock and contribute to landslide development (Margielewski & Urban, 2005).

Subhorizontally oriented zones of high resistivity in the depth exceeding 30 m could be found on longitudinal profiles LEM1-3, LEM4 and transverse profile LEM5. Existence of such structures have no reasonable geological explanation considering the subvertical dipping of flysch sedimentary layers, that are supposed to be continuous to considerable depth. Thus, these high resistivity zones could be artefacts of the inverse resistivity modelling because most of the interpretative programs works with the idea of the (sub)horizontally layered lithology (e.g. used Res2Dinv).

Local soils have very favourable characteristics to the slope deformation based on the soil samples analyses. They show very high content of clay and silt, which is very susceptible especially to the debris flow type forming (Easterbrook, 1999). That prove also Atterbergs limits with medium to high plasticity (Atkinson, 2007). Angle of internal friction of each soil sample was estimated much lower than the hillside slope, which was rather high, from 35° to 42°. Subsequently determined cohesion and cohesion at higher saturation may be used in a mathematical slope stability model. Consistency index came out high likely because the samples were taken out one year after the debris flow event and during dry season, so the soil close to the scarp could get hard under the climatic influence.

Previous mass movements in the area of interest could not be determined based on the dendrogeomorphological analysis because the trees were not available for sampling within the debris flow body. All the trees affected by 2010 debris flow were cut immediately after the event and were not available for the analysis. The 2010 debris flow is the only one known slope deformation from the study area during the analysed period 1/1983–10/2025, although heavier rainfall was recorded many times before 2010 and after. More than 50 records of the daily rainfall amount and API30 were higher, even double, than on 1st June 2010 (daily amount 37.3 m, API30 134.31 mm), but at the same time both characteristics were only three times above the 2010 debris flow volume and very close only four times (Tab. 5). These results indicate, that the combination of above-average daily and antecedent 30-day rainfall was more important for triggering the Lemešná debris flow than their extreme individual amounts. The same pattern with the combination of the daily totals and API30 (both parameters simultaneously above-average but not extreme) was recorded in the rainfall analyses of the debris flow on the Smědava Mt., Jizerské hory Mts. in 2010 (Smolíková et al., 2016). Hourly and 10-min. intensities were additionally available there, which distinguished only one day of the slope deformation (the combination of the above-average 10-min. and hourly intensities, daily totals and API30 at the same time). However, 10-minute and hourly intensities, which could make the analysis in this study more accurate, were not available from the VKP rainfall gauge.

The API for 60 and 90 days were not as significant as they had a very similar trend to the API30. Moreover, the API calculations for more than 60 days had the same results (137.5 for 60 days, 137.8 for 90 days), which is obtained by subtracting the evapotranspiration index from the rainfall totals. Thus, after 60 days, the rainfall total of the first calculation date was approaching zero.

Many authors determine rainfall thresholds that initiate slope deformation based on statistical analyses (e.g. Bíl & Müller, 2008; Corominas & Moya, 1999; Guzzetti et al., 2007; Krejčí et al., 2002; Rączkowski, 2007), but many of them deal only with individual rainfall parameters (e.g. Caine, 1980; Finlay et al., 1997; Glade, 1998; Guzzeti et al., 2008; Rebetez et al., 1997; Remaître & Malet, 2017; Rybář & Novotný, 2005), some of them with a combination of two calculations (e.g. Aristizábal et al., 2011; De Vita, 2000; Kim et al., 1991; Pasuto & Silvano, 1998;

Date	Rainfall daily amount [mm]	API30 [mm]
8 Aug 1985	65.5	165.4
26 Jun 1987	70.0	128.7
7 Sep 1996	83.5	132.5
6 Jul 1997	76.0	131.9
7 Jul 1997	70.0	187.8
8 Jul 1997	63.8	233.9
17 May 2010	33.7	147.5
1 Jun 2010 (DF)	**37.3**	**134.3**
31 Aug 2010	91.5	123.7
26 May 2014	75.8	98.2
14 Sep 2024	91.2	134.0

Tab. 5: Selected daily rainfall data and API30 higher than the rainfall volume of the debris flow event day
Notes: DF – debris flow event, grey highlighting – amounts higher than DF event
Source: Authors' calculations and elaboration based on rainfall data from the Czech Hydrometeorological Institute

Terlien, 1998), but a detailed study of the combination and mutual interaction of several individual rainfall characteristics has not been carried out. The results for the Lemešná debris flow show that the mutual combination of multiple rainfall parameters was more important for its occurrence than the extreme values of these parameters individually. Also, most studies do not consider days with the higher rainfall totals without slope deformation (Smolíková et al., 2016).

The data from the VKP and new one installed LEM in the foothill of the debris flow slope were compared. The distance between them is about 7 km under different orography, that affects the local conditions in mountainous terrain (Gysi, 1998). The maximum differences of the daily rainfall amount between them reached 37–71 mm (Tab. 4), however, 90% of the amounts reached a difference between 0–10 mm. According to Panziera et al. (2011) the distribution of the triggering rainfall varies across distances of up to 5 km, so the real triggering rainfall that caused the Lemešná debris flow might be significantly different. Indeed, rainfall data analysis is usually connected with many uncertainties like imprecise data, technical possibilities, manner of recording, rain gauge breakdown, lack of detailed data and statistical methods as well (Smolíková et al., 2016). Also, the rainfall is not the only causative factor for the slope deformation initiation in general (Aleotti & Chowdhury, 1999).

6. Conclusions

Slope deformations are a part of the long-term landscape development in the study area. There are suitable conditions for mass moving due to the flysch-type geological structure, steep slopes and heavy rainfalls, which is indicated by previous slope movement activity in the form of older slope deformations and two deposit cones. The last known event in the study area was the recent debris flow originated on 2nd June 2010, which caught a special attention there, because it affected family house and caused small damages in the forest. So, the detailed multidisciplinary research of the triggering conditions was carried out and the possibility of its reactivation in the future was investigated. Based on the processed analyses the following conclusions were found:

- The 2010 debris flow was primarily triggered by the combined effect of antecedent rainfall and daily precipitation totals. Rainfall analysis revealed that the above-average values of several rainfall parameters (1-day totals; cumulative totals for 2, 3, 4, 5, 10, 115, 20, 30, 60, 90 days; and API for 5, 10, 15, 20, 30, 60, 90 days) at the same time were more critical than extreme individual amounts of these parameters. However, indices higher than 60 days (API60 and higher) proved insignificant, as evapotranspiration reduced initial values toward zero, resulting in negligible variation in API90.
- Electrical resistivity tomography (ERT) revealed a thick layer of eroded colluvial material overlying subvertically bedded, heterogeneous flysch formations, which predispose the slope to deformation. The soil is dominated by fine-grained material (clay and silt), enhancing susceptibility to debris flow initiation. The debris flow base was identified at a depth of 5 m, with water accumulation above the source zone marking a critical point of origin. In addition, ERT detected a secondary sliding plane at 15–20 m depth, associated with an active crack above the scarp, suggesting the presence of a larger, currently inactive mass movement with potential for future reactivation. A distinct lithological boundary, likely a fault, was also recorded mid-slope (Fig. 7), further contributing to slope instability.
- Monitoring of slope activity in the study area using terrestrial laser scanner revealed minor surface changes by water erosion. Nevertheless, the survey should continue, because the possibility of the bigger slope deformation is rather high in the future.
- Soils are very susceptible to the slope deformation in the study area for their physical and index properties, especially for the high content of fine-grain material and even more in the combination with steep slope and additional water drained into the slope from the spring.
- Human interventions in this area, such as the inappropriate water drainage system and deforestation of the upper part of the slope in previous years before the 2010 debris flow, may have also significantly contributed to the failure.

The occurrence of the debris flow exclusively in 2010 could also have been influenced by other factors, such as short-interval rainfall intensities not recorded by VKP, differences between VKP and LEM totals under varying orographic conditions (different real local rainfall), long-term hydromechanical soil fatigue or others. Based on the available information, continued monitoring of the study area and its surroundings is highly recommended in the following years, due to the relatively high probability of further slope deformations. If further rainfall-induced slope deformations occur in this area, triggering rainfall could be analysed again and be more precisely identified. Local rainfall thresholds could be established.

Acknowledgement

We would like to thank the anonymous reviewers for their valuable comments, which significantly contributed to improving the quality of this paper. We are also grateful to the Czech Hydrometeorological Institute for providing the rainfall data essential to our analysis. Our special thanks go to Mr. and Mrs. Matyščák for their information and kind support in the study area. This work was supported by the project 'Natural and Anthropogenic Georisks' (CZ.02.01.01/00/ 22_008/0004605). The funding body had no influence in the design of the study, or the collection, analysis, and interpretation of data or in writing the manuscript.

References:

Abellán, A., Oppikofer, T., Jaboyedoff, M., Rosser, N. J., Lim, M., & Lato, M. J. (2014). Terrestrial laser scanning of rock slope instabilities. Earth Surface Processes and Landforms, 39, 80–97. https://doi.org/10.1002/esp.3493

Aleotti, P., & Chowdhury, R. (1999). Landslide hazard assessment: summary review and new perspectives. Bulletin of Engineering Geology and the Environment, 58, 21–44. https://doi.org/10.1007/s100640050066

Aristizábal, E., Martínez, H., & Velez, J. (2011). Analysis of empirical rainfall thresholds for the prognosis of landslides in the Aburrá Valley, Colombia. Revista EIA Escuela de Ingeniería de Antioquia, 15, 95–111.

Atkinson, J. H. (2007). The mechanics of soils and foundations. Routledge.

Bíl, M., Krejčí, O., Bílová, M., Kubeček, J., Sedoník, J., & Krejčí, V. (2014). A chronology of landsliding and its impacts on the village of Halenkovice, Outer Western Carpathians. Geografie, 119(4), 342–363. https://doi.org/10.37040/geografie2014119040342

Bíl, M., & Müller, I. (2008). The origin of shallow landslides in Moravia (Czech Republic) in the spring of 2006. Geomorphology, 99, 246–253. https://doi.org/10.1016/j.geomorph.2007.11.004

Burmister, D. M. (1940). Practical methods for the classification of soils. Proceedings of Purdue Conference on Soil Mechanics and its Applications. Purdue University.

Caine, N. (1980). The rainfall intensity-duration control of shallow landslides and debris flows. Geografiska Annaler, Series A(1–2), 62, 23–27. https://doi.org/10.2307/520449

Chlupáč, I. (2002). Geologická minulost České republiky. Academia.

Christoulas, S., Kalteziotis, N., Gassios, E., Sabatakakis, N., & Tsiambaos, G. (1990). Instability phenomena in weathered flysch in Greece. In C. Bonnard (Ed.), Landslides: Glissements de terrain, Vol. 1 (pp. 103–108). A. A. Balkema.

Corominas, J., & Moya, J. (1999). Reconstructing recent landslide activity in relation to rainfall in the Llobregat River basin, Eastern Pyrenees, Spain. Geomorphology, 30, 79–93. https://doi.org/10.1016/S0169-555X(99)00046-X

Corominas, J., & Moya, J. (2008). A review of assessing landslide frequency for hazard zoning purposes. Engineering Geology, 102, 193–213. https://doi.org/10.1016/j.enggeo.2008.03.018

Czech State Standards 731001 (1988). Foundation of structures. Subsoil under shallow foundations. Czech Office of Standards. (abolished in 2010)

Czech State Standards CEN ISO/TS 17892-1 (2015). Geotechnical investigation and testing, Laboratory testing of soil – Part 1: Determination of water content. Czech Office of Standards.

Czech State Standard CEN ISO/TS 17892-4 (2005). Geotechnical investigation and testing, Laboratory testing of soil – Part 4: Determination of particle size distribution. Czech Office of Standards. (abolished in 2017)

Czech State Standard CEN ISO/TS 17892-12 (2005). Geotechnical investigation and testing, Laboratory testing of soil – Part 12: Determination of Atterberg limits. Czech Office of Standards.

Del Prete, M., & Guadagno, F. M. (1990). Observations on landslides in typical flysch sequences of southern Apennines (Italy). In C. Bonnard (Ed.), Landslides: Glissements de terrain, Vol. 1. (pp. 109–113). A. A. Balkema.

De Vita, P. (2000). Fenomeni di instabilitŕ della coperture piroclastiche dei monti Lattari, di Sarno e di Salerno (Campania) ed analisi degli eventi pluviometrici determinanti. Quaderni di Geologia Applicata 7(2), 213–235.

Easterbrook, D. (1999). Surface processes and landforms. Prentice-Hall.

Finlay, P. J., Fell, R., & Meguire, P. K. (1997). The relationship between the probability of landslide occurrence and rainfall. Canadian Geotechnical Journal, 34, 811–824. https://doi.org/10.1139/t97-047

Földvary, G. Z. (1988). Geology of the Carpathian Region. World Scientific.

Gil, E. (1997). Meteorological and hydrological conditions of landslide, Polish Flysch Carpathians. Studia Geomorphologica Carpatho-Balcanica, 30, 144–158.

Glade, T. (1998). Establishing the frequency and magnitude of landslide-triggering rainstorm events in New Zealand. Environmental Geology, 35(2–3), 160–174. https://doi.org/10.1007/s002540050302

Guzzetti, F., Peruccacci, S., Rossi, M., & Stark, C. P. (2007). Rainfall thresholds for the initiation of landslides in central and southern Europe. Meteorology and Atmospheric Physics, 98, 239–267. https://doi.org/10.1007/s00703-007-0262-7

Guzzetti, F., Peruccacci, S., Rossi, M., & Stark, C. P. (2008). The rainfall intensity-duration control of shallow landslides and debris flows: An update. Landslides, 5(1), 3–17. https://doi.org/10.1007/s10346-007-0112-1

Gysi, H. (1998). Orographic influence of the distribution of accumulated rainfall with different wind directions. Atmospheric Research, 47–48(1), 615–633. https://doi.org/10.1016/S0169-8095(97)00089-6

Hungr, O., Leroueil, S., & Picarelli, L. (2014). The Varnes classification of landslide types, an update. Landslides, 11, 167–194. https://doi.org/10.1007/s10346-013-0436-y

Iverson, R. M. (1997). The Physics of Debris Flows. Reviews of Geophysics, 35, 245–296. https://doi.org/10.1029/97RG00426

Jakob, M., & Hungr, O. (2010). Debris-flow hazards and related phenomena. Praxis Publishing Ltd.

Janoška, M. (2013). Sopky a sopečné vrchy ČR. Academia.

Kim, S. K., Hong, W. P., & Kim, Y. M. (1991). Prediction of rainfall-triggered landslides in Korea. In D. H. Bell (Ed.), Landslides (pp. 989–994). A. A. Balkema.

Kirchner, K., Krejčí, O., Máčka, Z., & Bíl, M. (2000). Slope deformations in eastern Moravia, Vsetín District (Outer Western Carpathians). AUC XXXV, 133–143.

Klimeš, J. (2007). Analýza podmínek vzniku svahových deformací ve Vsetínských vrších. PhD thesis. Charles University in Prague.

Klimeš, J., Baroň, I., Pánek, T., Kosačík, T., Burda, J., Kresta, F., & Hradecký, J. (2009). Investigation of recent catastrophic landslides in the flysch belt of Outer Western Carpathians (Czech Republic): progress towards better hazard assessment. Natural Hazards and Earth System Sciences, 9, 119–128. https://doi.org/10.5194/nhess-9-119-2009

Klimeš, J., Stemberk, J., Blahůt, J., Krejčí, V., Krejčí, O., Hartvich, F., & Kycl, P. (2017). Challenges for landslide hazard and risk management in 'low risk' regions, Czech Republic – landslide occurrences and related costs (IPL project No. 197). Landslides, 14, 771–780. https://doi.org/10.1007/s10346-017-0798-7

Klimeš, J., & Vilímek, V. (2011). A catastrophic landslide near Rampac Grande in the Cordillera Negra, northern Peru. Landslides, 8, 309–320. https://doi.org/10.1007/s10346-010-0249-1

Kohler, M. A., & Linsley, R. K. (1951). Predicting the runoff from storm rainfall. Weather Bureau, US Department of Commerce, Research Paper, 34.

Kováčik, M. (1991). Slope deformations in the flysch strata of the West Carpathians. In D. H. Bell (Ed.), Landslides: Glissements de terrain, Vol. 1. (pp. 139–144). A. A. Balkema.

Krejčí, O., Baroň, I., Bíl, M., Hubatka, F., Jurová, Z., & Kirchner, K. (2002). Slope movements in the Flysch Carpathians of Eastern Czech Republic triggered by extreme rainfalls in 1997: A case study. Physics and Chemistry of the Earth, Parts A/B/C, 27(36), 1567–1576. https://doi.org/10.1016/S1474-7065(02)00178-X

Lenart, J., Pánek, T., & Dušek, R. (2014). Genesis, types and evolution of crevice-type caves in the flysch belt of the Western Carpathians (Czech Republic). Geomorphology, 204, 459–476. https://doi.org/10.1016/j.geomorph.2013.08.025

Loke, M. H. (1997). Electrical imaging surveys for environmental and engineering studies. A practical guide to 2-D and 3-D surveys.

Margielewski, W., & Urban, J. (2005). Pre-existing tectonic discontinuities in the rocky massifs as initial forms of deep-seated mass movements development: case studies of selected deep crevice-type caves in the Polish Flysch Carpathians. In K. Senneset, K. Flaate, & J. O. Larsen (Eds.), Landslides and avalanches ICFL 2005 Norway (pp. 249–256). Taylor & Francis.

Mishra, S. K., & Singh, V. P. (2003). Soil conservation service curve number (SCS-CN) methodology. Kluwer Academic Publisher. http://doi.org/10.1007/978-94-017-0147-1

Muńoz-Torrero Manchado A., Ballesteros-Cánovas, J. A., Allen, S., & Stoffel, M. (2022). Deforestation controls landslide susceptibility in Far-Western Nepal. Catena, 219, 106627. https://doi.org/10.1016/j.catena.2022.106627

Myslivec, A., Eichler, J., & Jesenák, J. (1970). Mechanika zemin. SNTL.

Nemčok, A., Pašek, J., & Rybář, J. (1972). Classification of landslides and other mass movements. Rock Mechanics 4. Springer-Verlag. https://doi.org/10.1007/BF01239137

Pánek, T., Hartvich, F., Jankovská, V., Klimeš, J., Tábořík, P., Bubík, M., ..., & Hradecký, J. (2014). Large Late Pleistocene landslides from the marginal slope of the Flysch Carpathians. Landslides, 11, 981–992. https://doi.org/10.1007/s10346-013-0463-8

Pánek, T., Hradecký, J., & Šilhán, K. (2009). Geomorphic evidence of ancient catastrophic flow type landslides in the mid-mountain ridges of the Western Flysch Carpathian Mountains (Czech Republic). International Journal of Sediment Research 24, 88–98. http://doi.org/10.1016/S1001-6279(09)60018-4

Pánek, T., & Lenart, J. (2016). Landslide landscape of the Moravskoslezské Beskydy Mountains and their surroundings. In T. Pánek, & J. Hradecký (Eds.), Landscapes and landforms of the Czech Republic. World geomorphological landscapes (pp. 347–359). Springer. http://doi.org/10.1007/978-3-319-27537-6_27

Pánek, T., Šilhán, K., Tábořík, P., Hradecký, J., Smolková, V., Lenart, J., ..., & Pazdur, A. (2011a). Catastrophic slope failure and its origins: Case of the May 2010 Girová Mountain long-runout rockslide (Czech Republic). Geomorphology, 130, 352–364. https://doi.org/10.1016/j.geomorph.2011.04.020

Pánek, T., Tábořík, P., Klimeš, J., Komárková, V., Hradecký, J., & Šťastný, M. (2011b). Deep-seated gravitational slope deformations in the highest parts of the Czech Flysch Carpathians: Evolutionary model based on kinematic analysis, electrical imaging and trenching. Geomorphology, 129, 92–112. https://doi.org/10.1016/j.geomorph.2011.01.016

Pánek, T., Tichavský, R., Březný, M., Galia, T., Kilnar, J., Tolasz, R., & Šustková, V. (2025). Debris flows triggered by storm Boris (September 2024) in the Czech Flysch Carpathians. Landslides, 22, 2493–2498. https://doi.org/10.1007/s10346-025-02526-7

Panziera, L., Germann, U., Gabella, M., & Mandapaka, P. V. (2011). NORA-nowcasting of orographic rainfall by means of analogues. Quarterly Journal of the Royal Meteorological Society, 137, 2106–2123. https://doi.org/10.1002/qj.878

Pasuto, A., & Silvano, S. (1998). Rainfall as a trigger of shallow mass movements. A case study in the Dolomites, Italy. Italian Journal of Engineering Geology and Environment, 35(2–3), 184–189. https://doi.org/10.1007/s002540050304

Pavelka, J., Trezner, J., et al. (2001). Příroda Valašska. ZO ČSOP Orchidea.

Preisig, G., Eberhardt, E., Smithyman, M., Preh, A., & Bonzanigo, L. (2016). Hydromechanical rock mass fatigue in deep-seated landslides

accompanying seasonal variations in pore pressures. Rock Mechanics and Rock Engineering, 49(6), 2333–2351. https://doi.org/10.1007/s00603-016-0912-5

Rączkowski, W. (2007). Landslide hazard in the Polish flysch Carpathians. Studia Geomorphologica Carpatho-Balcanica, XLI, 61–75.

Rebetez, M., Lugon, R., & Baeriswyl, P. A. (1997). Climatic change and debris flows in high mountain regions: the case study of the Ritigraben Torrent (Swiss Alp). Climatic Change, 36, 371–389. https://doi.org/10.1023/A:1005356130392

Remaître, A., & Malet, J. P. (2017). Regional rainfall thresholds for shallow and deep-seated mass movements triggering in the South-Eastern French Alps. In M. Mikoš, N. Casagli, Y. Yin, & K. Sassa (Eds.), Advancing culture of living with landslides. WLF 2017 (pp. 183–192). Springer. http://doi.org/10.1007/978-3-319-53485-5_20

Rybář, J., & Novotný, J. (2005). Vliv klimatogenních faktorů na stabilitu přirozených a antropogenních svahů. Zpravodaj Hnědé uhlí, 3, 13–28.

Schrott, L., & Sass, O. (2008). Application of field geophysics in geomorphology: Advances and limitations exemplified by case studies. Geomorphology, 93, 55–73. https://doi.org/10.1016/j.geomorph.2006.12.024

Segoni, S., Piciullo, L., & Gariano, S. L. (2018). A review of the recent literature on rainfall thresholds for landslides occurrence. Landslides, 15, 1483–1501. http://doi.org/10.1007/s10346-018-0966-4

Sidle, R. C. (1992). A theoretical model of the effects of timber harvesting on slope stability. Water Resources Research, 28, 1897–1910. https://doi.org/10.1029/92wr00804

Sidle, R. C. (2010). Influence of forest harvesting activities on debris avalanches and flows. In M. Jakob, & O. Hungr (Eds.), Debris flow hazards and related phenomena (pp. 363–409). Springer. https://doi.org/10.1007/3-540-27129-5_16

Sidle, R. C., & Ochiai, H. (2006). Landslides: processes, prediction, and land use. Water Resources Monograph, 18. American Geophysical Union. https://doi.org/10.1029/WM018

Šilhán, K., & Pánek, T. (2010). Fossil and recent debris flows in medium-high mountains (Moravskoslezské Beskydy Mts., Czech Republic). Geomorphology, 124, 238–249. http://doi.org/10.1016/j.geomorph.2010.03.026

Smolíková, J., Blahut, J., & Vilímek, V. (2016). Analysis of rainfall preceding debris flows on the Smědavská hora Mt., Jizerské hory Mts., Czech Republic. Landslides, 13(4), 683–696. https://doi.org/10.1007/s10346-015-0601-6

Smolíková, J., Hrbáček, F., Blahůt, J., Klimeš, J., Vilímek, V., & Loaiza Usuga, J. C. (2021). Analysis of the rainfall pattern triggering the Lemešná debris flow, Javorníky Range, the Czech Republic. Natural Hazards, 106, 2353–2379. https://doi.org/10.1007/s11069-021-04546-7

Špůrek, M. (1972). Historical catalogue of slide phenomena. Studia Geographica, 19.

Steinhart, M. (2010). Application of rainfall-runoff model Boussmo. Diploma thesis, Czech Agriculture University in Prague.

Šunka, Z., Sandev, M., Valeriánová, A. et al. (2011). Vyhodnocení povodní v květnu a červnu 2010, Souhrnná zpráva. Výzkumný ústav vodohospodářský T. G. Masaryka, v.v.i.

Táborík, P., Lenart, J., Blecha, V., Vilhelm, J., & Turský, O. (2017). Geophysical anatomy of counter-slope scarps in sedimentary flysch rocks (Outer Western Carpathians). Geomorphology, 2017, 59–70. http://doi.org/10.1016/j.geomorph.2016.09.038

Terlien, M. T. J. (1998). The determination of statistical and deterministic hydrological landslide-triggering thresholds. Environmental Geology, 35(2–3), 124–130. http://doi.org/10.1007/s002540050299

Tsukamoto, Y. (1990). Effect of vegetation on debris slide occurrences on steep forested slopes in Japan islands. International Association of Hydrological Sciences Publication, 192, 183–191.

Varnes, D. J. (1996). Landslides: Investigation and mitigation. Special report 247. National Academy Press. https://doi.org/10.17226/11057

Zavoral, J. et al. (1987). Metodiky laboratorních zkoušek v mechanice zemin a hornin. ČGÚ.

Please cite this article as:

Smolíková, J., Blahůt, J., Táborík, P., Klimeš, J., Žížala, D., Vilímek, V., ..., & Hartvich, F. (2026). Analysis of triggering factors of debris flows and conditions for possible reactivation: Case study of the Lemešná Mountain in the Javorníky Range, Czech Republic. Moravian Geographical Reports, 34(1), 46–59. https://doi.org/10.2478/mgr-2026-0004